RSC Advances

This is an *Accepted Manuscript*, which has been through the Royal Society of Chemistry peer review process and has been accepted for publication.

Accepted Manuscripts are published online shortly after acceptance, before technical editing, formatting and proof reading. Using this free service, authors can make their results available to the community, in citable form, before we publish the edited article. This *Accepted Manuscript* will be replaced by the edited, formatted and paginated article as soon as this is available.

You can find more information about *Accepted Manuscripts* in the Information for Authors.

Please note that technical editing may introduce minor changes to the text and/or graphics, which may alter content. The journal's standard Terms & Conditions and the Ethical guidelines still apply. In no event shall the Royal Society of Chemistry be held responsible for any errors or omissions in this *Accepted Manuscript* or any consequences arising from the use of any information it contains.

ROYAL SOCIETY OF CHEMISTRY

www.rsc.org/advances

Highly electrical conductivity of graphene-based transparent conductive films with silver nanocomposites

Haibin Sun[*ab], Guixian Ge[bc], Jiejun Zhu[bd], Hailong Yan[a], Yang Lu[a], Yaozheng Wu[b], Jianguo Wan[b], Min Han[b], and Yongsong Luo[*a]

[a]*Key Laboratory of Advanced Micro/Nano Functional Materials, Department of Physics and Electronic Engineering, Xinyang Normal University, Xinyang 464000, P. R. China*

[b]*National Laboratory of Solid State Microstructures, Department of Physics, Nanjing University, Nanjing 210093, P. R. China*

[c]*Key Laboratory of Ecophysics and Department of Physics, College of Science, Shihezi University, Xinjiang 832003, P. R. China*

[d]*School of Physics and Mathematical Sciences, Nanjing Tech University, Nanjing 211800, P. R. China*

E-mail: sunhaibin@xynu.edu.cn and ysluo@xynu.edu.cn

Abstract: Polycrystalline graphene films grown by chemical vapor deposition (CVD) possess outstanding electrical and optical properties, which make it alternative materials for applications in transparent conductive films (TCF). However, the high density of topological defects such as line dislocations and grain boundaries (GB) adversely affect the electrical conductivity of graphene films. Here, we find that silver nanocomposites (NC) consisting of nanowires and nanoparticles, which assembled with graphene to form a hybrid film can drastically decrease the sheet resistance (R_s) to 26 kΩ/sq comparable to that of the theoretical R_s of intrinsic graphene. Our results indicate that the graphene-based hybrid film is an alternative candidate for realizing high-performance TCF.

Keywords: Graphene, silver nanocomposites, transparent conductive films, hybrid films, sheet resistant

RSC Advances Accepted Manuscript

1. Introduction

Graphene has shown remarkable physical and chemical properties, such as high carrier mobility (up to 200000 $cm^2V^{-1}s^{-1}$), perfect optical transparency (97.7% at 550 nm), and impermeable to all gases.[1-3] These excellent properties of graphene can be maintained for a long time even under extreme stretching and bending in flexible and polymeric substrates, making graphene a potential candidate for transparent conductive films (TCF) to replace indium tin oxide (ITO). Large-scale graphene films using chemical vapor deposition (CVD) can be synthesized on metal surface and subsequently transferred to the arbitrary substrates.[4] A typical sheet resistance (R_s, >1 kΩ/sq) of CVD-grown graphene films is significantly higher than the intrinsic resistivity of graphene.[5,6] The main reason is the polycrystalline structure of CVD-grown graphene films with the high density of the topological defects such as line dislocations and grain boundaries (GB), which generate highly variable resistance as well as mechanical strength.[7]

Recently, several groups have proposed many methods to improve the optoelectronic properties of CVD-grown graphene films. The impressive result is that a hybrid film integrated silver nanowires (Ag NW) with a single layer graphene on a rigid glass substrate can obtain the R_s of 64±6.1 Ω/sq.[8] Furthermore, a high-performance TCF is assembled to form a subpercolating network consisting of graphene and Ag NW, in which the R_s of 32.5 Ω/sq.[9] Nevertheless, micrometer-sized holes within the network increase NW-NW contact resistance, resulting in the relatively higher R_s in the hind-end application of TCF (typically, R_s = 10-30 Ω/sq). In a recent paper by Hu et al., a network of Ag NW can decrease the overall resistance approximately two orders of magnitude by an Au nanoparticles (NP) coating process.[10] With this insight, metal NW and NP will provide a promising application for graphene-based TCF, and thus research on the interaction between NW, NP, and graphene hybrid films is well worthy prospect.

In this study, we fabricated a highly conductive graphene-based transparent hybrid film by transferring a CVD-grown bilayer graphene film onto a subpercolating Ag nanocomposites (NC) consisting the NW and NP. We show that the R_s of graphene films is drastically decreased to 26 Ω/sq by the Ag NC films. Based on the observations of surface topographies and measurements of optoelectronic properties of the hybrid films, we demonstrate that the metal Ag NC greatly improve the conductivity of the polycrystalline CVD-grown graphene films by bridging the topological defects with Ag NW and reducing the NW-NW contact resistance with Ag NP. On the basis of experimental results, we look far

RSC Advances Accepted Manuscript

ahead into the future that graphene/Ag NC hybrid films can be applied for emerging optoelectronic devices such as flexible touch panels, displays, and solar cells.

2. Experimental

2.1. Synthesis of Ag NC films

Ag nanocomposites (NC) consist of nanowires (NW ～40%, average length and diameter of 6-10 μm and 100-160 nm) and nanoparticles (NP ～60%, average diameter of 200 nm), which were synthesized by an improved polyol process.[11] A mixture of 0.2664 g of poly-vinylpyrrolidone (PVP; 17k, Boai New Kaiyuan Pharmacy) and 0.408 g of silver nitrate ($AgNO_3$; 99.8%, Sinopharm Chemical Reagent) was respectively solved in a 10 mL of ethylene glycol (EG; 99.5%, Nanjing Chemical Reagent) solvent. All chemical reagents and solvents were analytical grade without further purification. Both solvents were simultaneously injected dropwise into 40 mL of EG solvent which was heated and thermally stabilized at 150 ℃ in a round-bottomed flask. The 150 ℃ is a high enough temperature to enhance the reducing power of EG but below the boiling temperature of EG (197 ℃). The reaction time lasted about 80 min. Magnetic stirring was applied throughout the entire synthesis process. The cooled-down solution was diluted about fivefold by acetone and then centrifuged three times at 8000 rpm for 15 min to remove solvent (EG), PVP, and other impurities in the supernatant. After the final centrifugation, the precipitate of Ag NC was redisposed in 30 mL of methanol solution. For comparison, we selected different average molecular weight (MW) of PVP as a shape-directing surfactant to fabricate the Ag NP films and Ag NW films.

2.2. Synthesis of CVD bilayer graphene films

A large-scale bilayer graphene film was synthesized on a Cu foil by a nonisothermal atmospheric pressure chemical vapor deposition method.[12] Cold-rolled 1cm^2 Cu foil with a thickness 25 μm (99.8%, Alfa Aesar) was located into the center of horizontal quartz tube. The temperature rose to 1000 ℃ in the mixtures of Ar and H_2 with a total flow rate of 300 sccm, and then annealed for 30 min. Subsequently, 1.2 sccm CH_4 gases were passed through the quartz tube for 5 min to prepare the bilayer graphene films, accompanying with the cooling growth rate of 20 ^oC/min from 1000 ℃ to 900 ℃, and then the furnace was quickly cooled down to room temperature in the protection gases of Ar and H_2. After CVD-graphene growth, a wet transfer method is used to peel off graphene film from Cu foil to glass or SiO_2/Si substrates.[13] Namely, Cu foil was spin-coated with a thin layer of poly (methyl methacrylate) (PMMA), and put into the 1.0 M $FeCl_3$ etchant solution for 2 h to completely

RSC Advances Accepted Manuscript

etch away the Cu foil. And then the floated PMMA/graphene film was put into the deionized water for 30min. Later on, the film was scooped out by the target substrates and dried in air over night. In the end, the PMMA layer was removed by hot acetone.

2.3. Fabrication of the graphene/Ag NC hybrid films

To fabricate the graphene/Ag NC hybrid films, Ag NC films were prepared by spin-coating on glass or SiO_2/Si substrates. Three different concentrations of Ag NC films were obtained by diluting NC dispersions in deionized water: 0.8 mg/ mL, 0.5 mg/ mL, and 0.2 mg/mL, respectively. The corresponding films were denoted as NC1, NC2, and NC3. Subsequently, the PMMA-coated graphene was slowly lifted by Ag NC films, forming the PMMA/graphene/Ag NC hybrid films, and then were dried by air. The PMMA was completely removed by hot acetone to form the final hybrid films. Previously, our group has reported[14] that graphene film can firmly wrap the Ag NP and suppress their movement on glass or SiO_2/Si substrates, resulting in the increased contact area between the graphene and Ag NP. Thus, the dispensability of Ag NC and conductivity of graphene are unacted on the surfactants used in the synthesis of Ag NC films. Experimental section for the detailed information is illustrated in Fig. 1.

2.4. Characterization

The surface morphologies of the films were carried out by scanning electron microscopy (SEM) with a Sirin 200 SEM at 20 kV, transmission electron microscopy (TEM) and selected area electron diffraction (SAED) with a Tecnai G2 F20 field emission gun TEM at 200kV. Structural characteristics of the Ag NC films were obtained by X-ray diffraction (XRD) on a D/MAX-RA diffractometer using Cu Kα radiation. Raman spectroscopy analysis was used on Ntegra Spectroscopy Nanolaboratory with an excitation wavelength of 633 nm and a 100× objective lens. Optical transmittance spectra were recorded in the 200-1100 range by an ultraviolet-visible (UV-VIS)-NIR (U-3410; Hitachi, Tokyo, Japan) spectrophotometer. Electrical resistivity of the films was measured with a digital multimeter (Keithley 2400).

3. Results and discussion

Figure 2(a) shows the surface topography of Ag NC films transferred onto the SiO_2/Si substrates by the SEM image, indicating that Ag NC films are the mixed nanostructures with nanowires and nanoparticles. The inset of Fig. 2(a) shows that lots of Ag NP are filling the hollow in the NW. The phase purity of the products can be characterized by X-ray diffraction in the range from 30^o to 80^o. Figure 2(b) displays the typical diffraction pattern of products.

RSC Advances Accepted Manuscript

No additional peaks of impurities are detected from this pattern. The strongest and sharpest peak at 38.2° is the (111) plane of face-centered-cubic (fcc) Ag.[15] The other weak peaks are clearly observed at 2θ values of 44.38°, 64.26° and 77.46°, which are corresponding to the reflections of the (200), (220), and (311) crystal planes of metallic Ag, respectively.[9, 15] The calculated lattice constant from the XRD pattern is 4.062 Å, close to the reported data (α=4.086 Å, JCPDS file no. 04-0783).[16] This results indicate that the pure Ag nanostructures obtained are well crystallized structure under the present prepared methods.

Figure 2(c) shows a SEM image of the CVD-grown graphene film transferred onto the SiO_2/Si substrates. We can easily observe a typical graphene film with the uniform color contrast, but it also exhibits a high density of dark line distributions, such as wrinkles, folds, ripples, and GB, indicating that the growth and transfer process generate the additional line disruptions in graphene films. The microstructure and quality of the graphene films were further characterized by Raman spectroscopy. A typical Raman spectrum is shown in Fig. 2(d). The 2D and G peaks centered at ~2648 cm^{-1} and ~1587cm^{-1}, respectively. The corresponding intensity ratio of 2D and G peaks in this spectrum (I_{2D}/I_G) is ~1.0, meanwhile, the full width at half-maximum (fwhm) of the 2D peak is around 44 cm^{-1}, associating with bilayer graphene film.[12,17] In addition, the Raman D peak of graphene is observed at ~1350 cm^{-1}, which is attributed to the activated line defects due to the second-order scattering process including a defect and a phonon.[18]

To further demonstrate the characteristics for bilayer graphene film, we transferred the graphene film onto TEM lacey carbon-coated grids to observe a high-resolution TEM image and selected area electron diffraction (SAED) pattern. Figure 3 (a) shows a high-resolution TEM image of graphene film on the TEM grid. It is clearly seen that two-layer folded edge confirms the thickness of the bilayer graphene film. Corresponding to the blue circle region in Fig 3(a), SAED pattern shows one set of six-fold symmetry arrangement of carbon atoms. In the SAED pattern, the outer {1–210} peak intensity was 2.0 times stronger than the inner {–1100} peak intensity in Fig 3(b-c), suggesting that the graphene is single-crystal and bilayer graphene is AB-stacked.[12,17]

A hybrid film, integrating graphene with Ag NC, is shown schematically in Fig. 1. Here, Ag NC films are diluted by the deionized water to form the nonconductive subpercolation networks, indicating that NC films are individual and local distribution. In virtue of the discrete distribution of Ag NC films, it can not only individually provide the conductive paths but also greatly reduce the contact resistances of wire-to-wire relative to the dense

RSC Advances Accepted Manuscript

crossed NW, resulting in the improving electrical conductivity of graphene by the nonconductive Ag NC films.[8] This result is different from those reported by Tour et al.[19] for graphene transferred onto a metallic grid, where the continuous graphene and metallic grid are all contributed to the global electrical conductivity. In the final graphene/Ag NC hybrid sample, it was found that suspended graphene traps liquid and nanoparticles around the Ag nanowires (Fig. 4b), resulting in poor transport properties of the hybrid sample. To avoid the presence of the suspended graphene, a redissolution PMMA method[8] was used to form the PMMA/PMMA/graphene/Ag NC hybrid film, as shown in Fig. 4a. The second layer of PMMA solution can dissolve the precoated PMMA layer and obtain a better contact to the surface morphology between graphene and the Ag NC films. After putting at room temperature for a few minutes, two-layer PMMA films were removed by hot acetone. Finally, the suspended graphene has not been observed in the graphene/Ag NC hybrid films from the SEM image (Fig. 4c). The modified hybrid preparation process can allow the graphene to conform to the curvature of the underlying Ag NC films, enhancing interfacial contact area between graphene and NC, further improving the conductivity of the hybrid films.

The graphene and graphene/Ag NC hybrid films with three different concentrations prepared onto the SiO_2/Si substrates are illustrated by the SEM images in Fig. 5(a-f). In comparison with Fig. 2(a), the concentrations of Ag NC films were diluted by the deionized water. The different concentrations of hybrid films induce the various conductivity of the graphene films. In addition, the hybrid films were a loss of Ag NC concentrations during the transfer process of the graphene films, which is due to scooping out the graphene films from a liquid environment for a few seconds. The final graphene-veiled-Ag NC structures have a good thermal stability because the flexible graphene films can firmly wrap the Ag NC films and thereby it is difficult for Ag NC films to move, resulting in the stable contact area between graphene and Ag NC films. Meanwhile, many research groups have found that too long exposure of Ag in the atmospheric environment would dramatically diminish optical and electrical properties because of oxidizing and sulfurizing reaction with the surface of Ag.[20,21] While the inert graphene film can passivate the surface of Ag by blocking diffusion of gas molecules, protecting its excellent optoelectronic properties.[14] Thus, graphene/Ag NC hybrid films based TCF applications can be significantly more stable and useful even over a long time period.

The optoelectronic properties of the graphene and graphene/Ag NC hybrid films were performed to measure and compare with each other. In the Figure 5(g), the transmittances of

RSC Advances Accepted Manuscript

the hybrid films transferred onto the glass substrates are measured by an ultraviolet-visible spectrophotometer, which are demonstrated that the transmittances of hybrid films dramatically reduce due to the added layer of the Ag NC films. The transmittance of graphene/Ag NC3 hybrid film reaches up to 93.1% at 550 nm, which is the higher than that of the other hybrid films. The relatively low transmittances of the other hybrid films are not problematic in voltage-based devices such as liquid crystal displays and capacitive touch screens. Based on the SEM images in Fig. 5(b-f), we found the presence of an excess of nanoparticles and nanowires in the hybrid films, which can be regarded as the major reasons for the reduction of transmittance in the hybrid films.

In addition, the R_s of the graphene and graphene/Ag NC hybrid films transferred onto the SiO_2/Si substrates was measured using an Alessi four-point probe method without additional annealing treatment. Figure 5(h) shows that the R_s of the prepared hybrid films significantly reduces from NP to NC1, which are all lower than that of CVD-grown graphene films. The lowest sheet resistance (R_s=26 Ω/sq) is obtained from the graphene/Ag NC1 hybrid film, which is comparable to the intrinsic resistivity of perfect graphene (30 Ω/sq for graphene/SiO_2/Si system).[6] The low sheet resistance obtained confirms that Ag NC films can strongly decrease the electrical resistance of CVD-grown polycrystalline graphene films by repairing the line defects (such as GB, wrinkles). In contrast, the sheet resistances of graphene/Ag NP graphene/Ag NW hybrid films show the low R_s but even higher than the intrinsic resistivity of perfect graphene.

In order to obtain the high-performance TCF with the lowest sheet resistance as well as the highest optical transmittance from the hybrid films, the interrelation between optical transmittance and sheet resistance of a thin conductive film can be written as[9]

$$FoM = \frac{188.5}{R_s} \cdot \left(\frac{\sqrt{T(\lambda)}}{1-\sqrt{T(\lambda)}} \right) \quad (1)$$

where figure-of-merit (FoM) is commonly used to quantify the material properties of DC conductivity and optical conductivity at 550 nm. In the previous reports for metal nanowires, carbon nanotube and graphene used as TCF, the accuracy of this expression has been sufficiently demonstrated.[22-24] Based on the above analysis, the value of FoM can be regarded as a criterion to evaluate the performance of TCF. In our study, the lowest R_s = 26 Ω/sq was obtained from the graphene/NC1 hybrid film, and its FoM is 63.1 (Fig. 6). It is clear that the FoM of graphene/NC1 hybrid film is much higher than that of graphene/Ag NP

RSC Advances Accepted Manuscript

and graphene/Ag NW hybrid films. Thus, we believe that the engineering of graphene by Ag NC films is more effective strategy for realizing high performance graphene-based TCF.

In consideration of the subpercolating network of Ag NC films, we conclude that Ag NC films have the dual roles in improving the electrical conductivity of the CVD-grown graphene films: (1) to bridge GB and line disruptions of the CVD-grown polycrystalline graphene films by Ag NW, a convention method to improve the conductivity of graphene; and (2) to aggregate around Ag NW randomly and enhance tight connections between NW by NP. This is similar to the role of gold NP coating on the network of Ag NW: formed silver-gold alloyed nanowires drastically decrease the NW-NW contact resistance.[10] Figure 2(a) shows a typical SEM image of the Ag NC films, in which NP tightly contact with NW. Among the SEM images of the hybrid films (Fig.5 b-f), it is notable that many Ag NP exist in the crossed Ag NW positions to link up with the crossed NW. Thus, Ag NP is mainly due to the reduction in contact resistance of NW-NW. In addition, the continuous graphene films provide a long-range electron transport pathway between NW and NP, forming the global conductive hybrid films.

Recently, graphene-based composites as TCF were widely reported,[9,15] where the graphene/Ag NW hybrid films were prepared on the 300 μm thick polyethylene terephthalate (PET) substrate, replacing ITO glass substrate for application in the flexible solar cells as well as excellent optical transparency and electric conductivity. Given an ordered pattern of the NP or NW on graphene that can be prepared using capillary forces, [25,26] we look forward to get the superior conductivity and perfect transmittance of graphene based TCF in the next work.

4. Conclusion

In summary, we experimentally prepared the graphene/Ag NC hybrid films on SiO_2/Si substrates to obtain excellent electrical property for a sheet resistance (26 Ω/sq), exceeding the intrinsic resistance of perfect graphene. This is achieved *via* applying Ag NC films to improve electrical conductivity of the polycrystalline graphene films. While graphene films act as a continuous film to provide the global conductivity of the nonconductive Ag NC films. It is demonstrated that the joint effect of 2D graphene film with 1D metal NC can significantly decrease the global resistance of the hybrid films. The integration of such graphene/metal NC hybrid film as TCF shows its excellent electrical performance, indicating the potential feasibility for replacing ITO in a broad range of applications including flexible electronics, photovoltaics, and energy storage.

RSC Advances Accepted Manuscript

Acknowledgments

This work was financially supported by the National Natural Science Foundation of China (Grant No. 51472113, 21403144, 11464038, U1204501, U1304108), and program of the Innovative Research Team (in Science and Technology) in University of Henan Province (No. 13IRSTHN018), program for Science & Technology Innovation Talents in University of Henan Province (No. 15HSTIT018), program for Natural Science Research of Henan Province Education Department (No. 2011B450002).

RSC Advances Accepted Manuscript

References

1 K. S. Novoselov, A. K. Geim, S. V. Morozov, D. Jiang, Y. Zhang, S. V. Dubonos, I. V. Grigorieva, and A. A. Firsov, *Science*, 2004, **306**, 666-669.

2 R. R. Nair, P. Blake, A. N. Grigorenko, K. S. Novoselov, T. J. Booth, T. Stauber, N. M. R. Peres, and A. K. Geim, *Science*, 2008, **320**, 1308.

3 S. S. Chen, L. Brown, M. Levendorf, W. W. Cai, S. Y. Ju, J. Edgeworth, X. S. Li, C. W. Magnuson, A. Velamakanni, R. D. Piner, J. Y. Kang, J. Park, and R. S. Ruoff, *ACS Nano*, 2011, **5**, 1321-1327.

4 X. S. Li, W. W. Cai, J. An, S. Kim, J. Nah, D. X. Yang, R. Piner, A. Velamakanni, I. Jung, E. Tutuc, S. K. Banerjee, L. Colombo, and R. S. Ruoff, *Science*, 2009, **324**, 1312-1314.

5 K. S. Kim, Y. Zhao, H. Jang, S. Y. Lee, J. M. Kim, K. S. Kim, J. H. Ahn, P. Kim, J. Y. Choi, and H. Hong, *Nature*, 2009, **457**, 706-710.

6 J. H. Chen, C. Jang, S. D. Xiao, M. Ishigami, and M. S. Fuhrer, *Nat. Nanotechnol.*, 2008, **3**, 206-209.

7 A. W. Tsen, L. Brown, M. P. Levendorf, F. Ghahari, P. Y. Huang, R. W. Havener, C. S. Ruiz-Vargas, D. A. Muller, P. Kim, and J. Park, *Science,* 2012, **336**, 1143-1146.

8 I. N. Kholmanov, C. W. Magnuson, A. E. Aliev, H. F. Li, B. Zhang, J. W. Suk, L. L. Zhang, E. Peng, S. H. Mousavi, A. B. Khanikaev, R. Piner, G. Shvets, and R. S. Ruoff, *Nano Lett*., 2012, **12**, 5679-5683.

9 Y. Liu, Q. H. Chang, and L. Huang, *J. Mater. Chem. C*, 2013, **1**, 2970-2974.

10 L. B. Hu, H. S. Kim, J. Y. Lee, P. Peumans, and Y. Cui, *ACS Nano*, 2010, **4**, 2955-2963.

11 J. J. Zhu, C. X. Kan, J. G. Wan, M. Han, and G. H. Wang, *J. Nanomater*., 2011, **2011** 982547.

12 H. B. Sun, J. Wu, Y. Han, J. Y. Wang, F. Q. Song, and J. G. Wan, *J. Phys. Chem. C*, 2014, **118**, 14655-14661.

13. X. S. Li, Y. W. Zhu, W. W. Cai, M. Borysiak, B. Y. Han, D. Chen, R. D. Piner, L. G. Colombo, and R. S. Ruoff, *Nano Lett.*, 2009, **9**, 4359-4363.

14 H. B. Sun, J. Wu, J. J. Zhu, D. F. Pan, G. H. Wang, and J. G. Wan, *Appl. Phys. Lett.*, 2015, **106**, 211603.

15 S. C. Xu, B. Y. Man, S. Z. Jiang, M. Liu, C. Yang, C. S. Chen, and C. Zhang, *CrystEngComm*. 2014, **16**, 3532-3539.

16 P. Mohanty, I. Yoon, T. Kang, K. Seo, K. S. K. Varadwaj, W. Choi, Q. H. Park, J. P. Ahn, Y. D. Suh, H. Ihee, and B. Kim, *J. Am. Chem. Soc.*, 2007, **129**, 9576-9577.

17 L. X. Liu, H. L. Zhou, R. Chen, W. J. Yu, Y. Liu, Y. Chen, J. Shaw, X. Zhong, Y. Huang, and X. F. Duan, *ACS Nano*, 2012, **6**, 8241-8249.

18 A. C. Ferrari, and D. M. Basko, *Nat. Nanotechnol.*, 2013, **8**, 235-246.

19 Y. Zhu, Z. Z. Sun, Z .Yang, Z. Jin, and J. M. Tour, *ACS Nano*, 2011, **5**, 6472-6479.

RSC Advances Accepted Manuscript

20 M. Losurdo, I. Bergmair, B. Dastmalchi, T. H. Kim, M. M. Giangregroio, W. Y. Jiao, G. V. Bianco, A. S. Brown, K. Hingerl, and G. Bruno, *Adv. Funct. Mater.*, 2014, **24**, 1864-1879

21 J. C. Reed, H. Zhu, A. Y. Zhu, C. Li, and E. Cubukcu, *Nano Lett.*, 2012, **12**, 4090-4094.

22 L. J. Andrés, M. F. Menéndez, D. Gómez, A. L. Martínez, N. Bristow, J. P. Kettle, A. Menéndez, and B. Ruiz, *Nanotechnology*, 2015, **26**, 265201.

23 H. Jung, J. S. Yu, H. P. Lee, J. M. Kim, J. Y. Park, and D. Kim, *Carbon*, 2013, **52**, 259-266.

24 S. De, and J. N. Coleman, *ACS Nano*, 2010, **4**, 2713-2720.

25 Y. Zhou, X. Z. Zhou, D. J. Park, K. Torabi, K. A. Brown, M. R. Jones, C. Zhang, G. C. Schatz, and C. A. Mirkin, *Nano Lett.*, 2014, **14**, 2157-2161.

26 X. Z. Zhou, Y. Zhou, J. C. Ku, C. Zhang, and C. A. Mirkin, *ACS Nano*, **8**, 1511-1516.

RSC Advances Accepted Manuscript

Figure Captions

Fig. 1. Process flow illustrating the fabrication of a graphene/Ag NC hybrid film on 300 nm SiO_2/Si substrate.

Fig. 2. Characteriztion of Ag NC and CVD-grown graphene. (a) SEM image of the original Ag NC coated on a SiO_2/Si substrate. Inset shows the enlarged SEM image obtained from the random position in (a). (b) XRD spectrum of Ag NC corresponding to (a). (c) SEM image of graphene transferred onto a SiO_2/Si substrate. The arrows show the line defects (such as GB, ripples, folds and wrinkles). (d) Raman spectrum corresponding to the random area in (c).

Fig. 3. (a) High resolution TEM image of the graphene film. (b) SAED patterns taken from the blue circle-shape region in (a). (c) Profile plots of diffraction peak intensities along the arrows (from down to top) in (b).

Fig. 4. Preparation of graphene/Ag NC hybrid films. (a) Schematic illustration of modified hybrid film preparation method. (b) SEM image of the original grphene wet-transferred onto Ag NC film. (c) SEM image of graphene/Ag NC film after redissolving PMMA method.

Fig. 5. (a-f) SEM images of the graphene and graphene/Ag NC hybrid films. (g) Optical transmittance spectra of graphene and graphene/ Ag NC hybrid films. (h) Sheet resistance versus optical transmittance for graphene and graphene/ Ag NC hybrid films.

Fig. 6. Comparison of FoM between graphene and graphene/ Ag NC hybrid films.

RSC Advances Accepted Manuscript

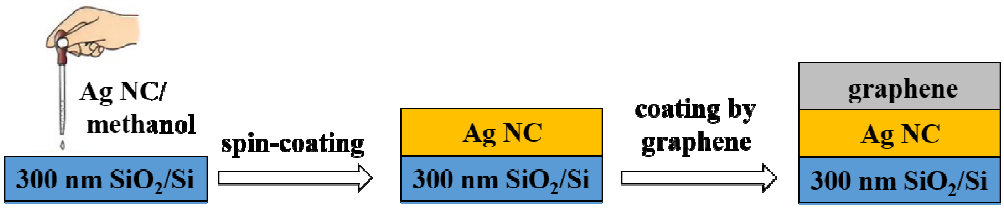

Fig 1

RSC Advances Accepted Manuscript

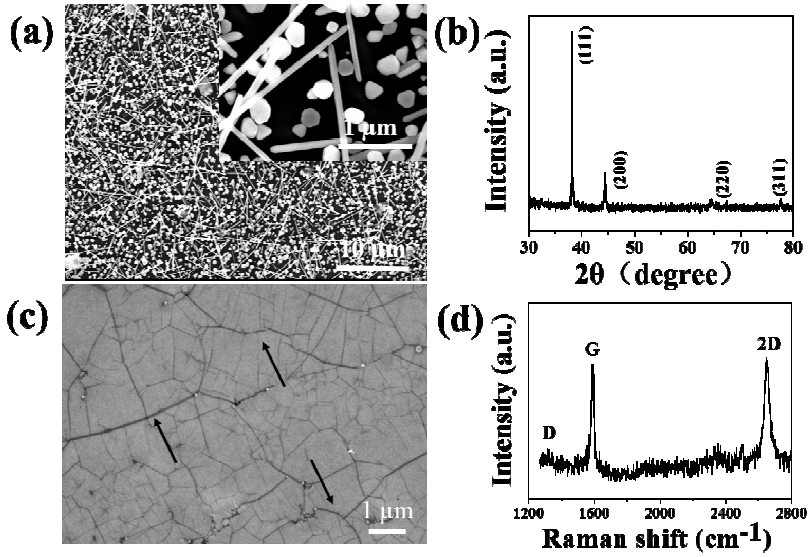

Fig 2

RSC Advances Accepted Manuscript

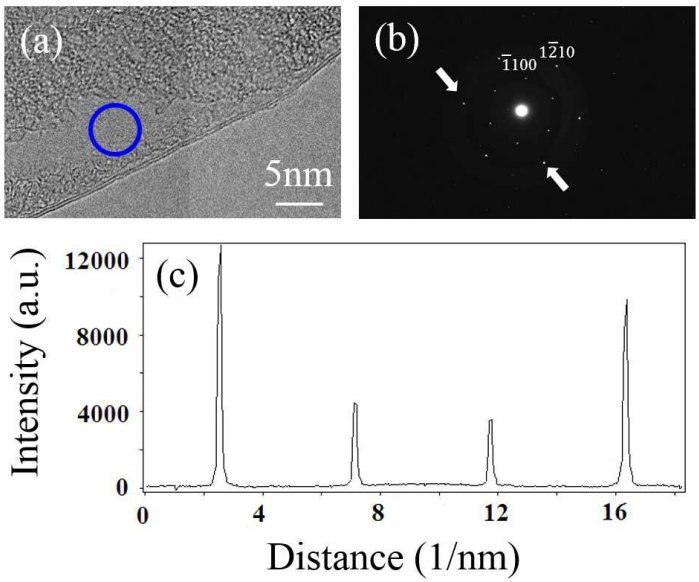

Fig 3

RSC Advances Accepted Manuscript

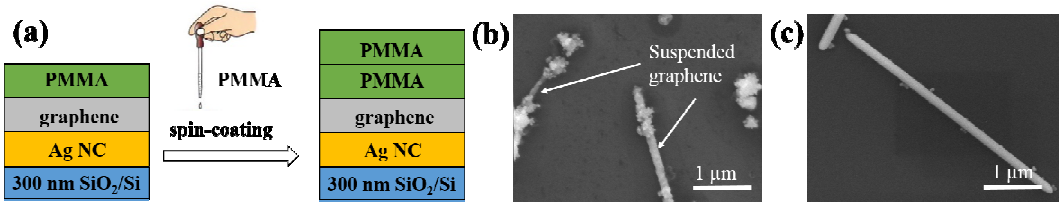

Fig 4

RSC Advances Accepted Manuscript

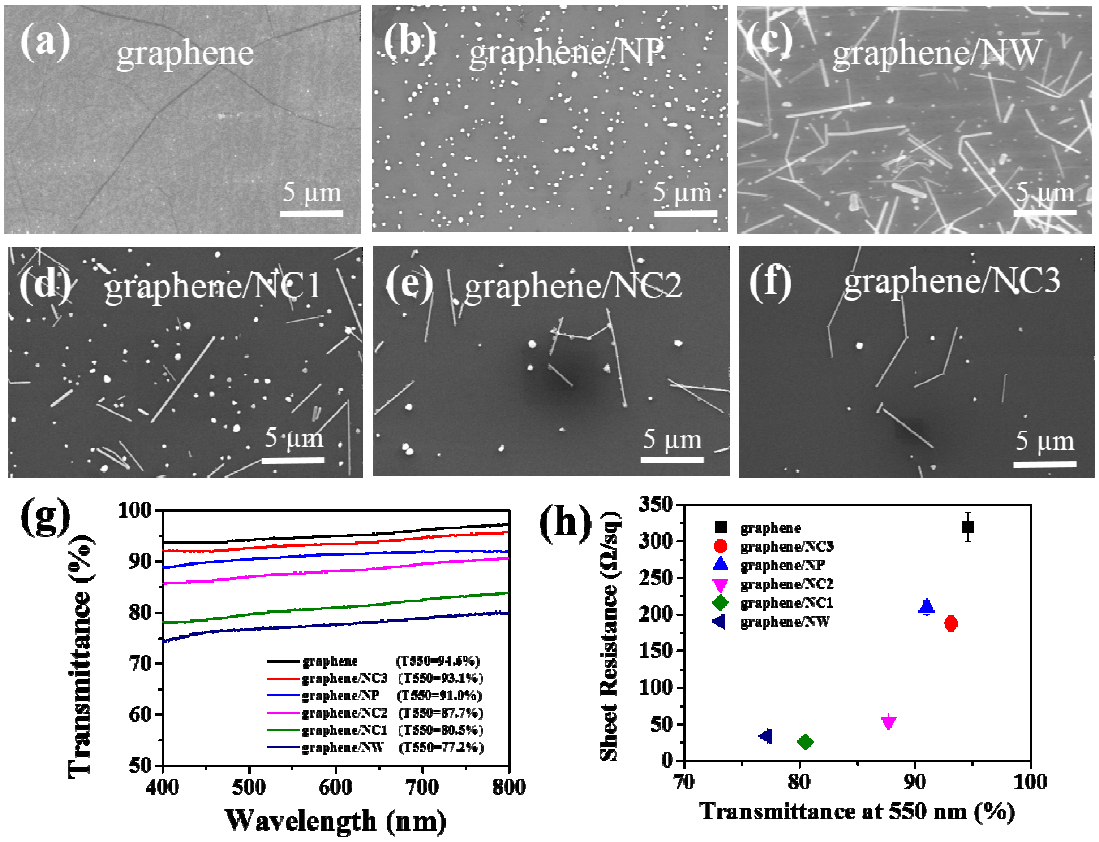

Fig 5

RSC Advances Accepted Manuscript

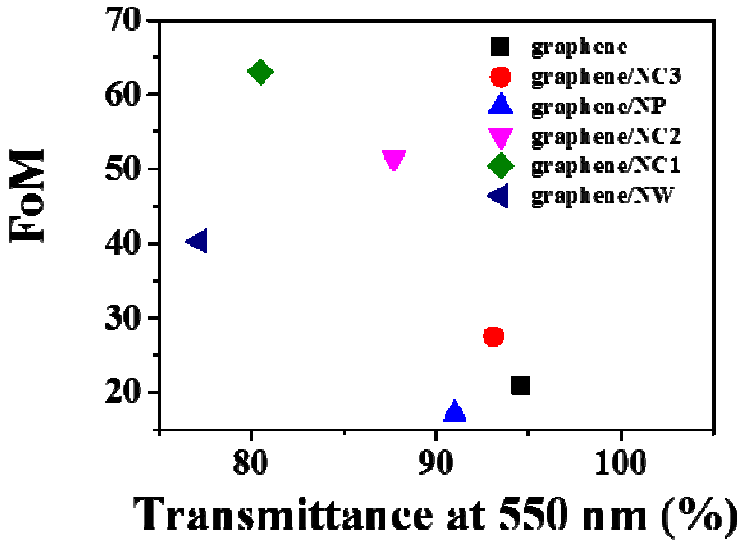

Fig 6

RSC Advances Accepted Manuscript